ORIGINAL RESEARCH

Glycosaminoglycan Overproduction in the Aorta Increases Aortic Calcification in Murine Chronic Kidney Disease

Eko Purnomo, MD; Noriaki Emoto, MD, PhD; Dwi Aris Agung Nugrahaningsih, MD, MSc; Kazuhiko Nakayama, MD, PhD; Keiko Yagi, MD, PhD; Susi Heiden, DVM; Satomi Nadanaka, PhD; Hiroshi Kitagawa, PhD; Ken-ichi Hirata, MD, PhD

***Background*—**Vascular calcification accompanying chronic kidney disease increases the mortality and morbidity associated with cardiovascular disorders, but no effective therapy is available. We hypothesized that glycosaminoglycans may contribute to osteoblastic differentiation of vascular smooth muscle cells during vascular calcification.

***Methods and Results*—**We used exostosin-like glycosyltranferase 2–deficient (*EXTL2* knockout) mice expressing high levels of glycosaminoglycans in several organs including the aorta. We performed 5/6 subtotal nephrectomy and fed the mice a high-phosphate diet to induce chronic kidney disease. Overexpression of glycosaminoglycans in the aorta enhanced aortic calcification in chronic kidney disease in *EXTL2* knockout mice. Ex vivo and in vitro, matrix mineralization in aortic rings and vascular smooth muscle cells of *EXTL2* knockout mice was augmented. Furthermore, removal of glycosaminoglycans in *EXTL2* knockout and wild-type mice-derived vascular smooth muscle cells effectively suppressed calcium deposition in a high-phosphate environment.

***Conclusions*—**These results illustrate an important role for glycosaminoglycans in the development of vascular calcification. Manipulation of glycosaminoglycan expression may have beneficial effects on the progression of vascular calcification in chronic kidney disease patients. **(*J Am Heart Assoc.* 2013;2:e000405 doi: 10.1161/JAHA.113.000405)**

Key Words: chondroitin sulfate • chronic kidney disease • glycosaminoglycan • heparan sulfate • vascular calcification

Vascular calcification accelerates the progression of cardiovascular disorders in patients with chronic kidney disease (CKD).[1] Calcification of blood vessels reduces their elasticity and promotes arterial stiffness and increases blood and pulse pressure and the risk of heart failure.[2–4] Current therapeutic strategies for vascular calcification focus on correction of the disordered bone and mineral metabolism that accompanies CKD.[5] Vitamin D receptor agonists and calcimimetics provide survival benefits and delay the progression of vascular calcification, respectively.[6,7] In addition, controlling the serum phosphate level using phosphate binders, sevelamer, and lanthanum offers the advantage of a low incidence of vascular calcification in CKD patients.[8,9] However, despite the improvement of cardiovascular function and structure by sevelamer hydrochloride, other studies failed to demonstrated a significant difference in the progression of vascular calcification between calcium acetate and sevelamer hydrochloride. Furthermore, inconsistent results of sevelamer effects on mortality in heart disease patients have been shown in some studies.[10] Even though several potential therapies that directly ameliorate vascular calcification have presented beneficial effects in animal and human studies,[11] the effects of these therapies appear to be insufficient; therefore, no effective regiment is currently available for the treatment of vascular calcification.[12] A deeper understanding of vascular calcification mechanisms is strongly necessary to provide novel strategies for the treatment of vascular calcification in CKD patients.

Vascular smooth muscle cells (VSMCs) represent the predominant cell type in the arterial walls and actively transdifferentiate into an osteoblastic/chondrocytic-like phenotype during the development of vascular calcification.[13,14] Similar to bone cells, transdifferentiated VSMCs express osteoblastic differentiation factors such as runt-related transcription factor 2, osteopontin, and matrix gla protein,

From the Division of Cardiovascular Medicine, Department of Internal Medicine, Kobe University Graduate School of Medicine, Kobe, Japan (E.P., N.E., D.A.A.N., K.H.); Departments of Clinical Pharmacy (N.E., K.N., K.Y., S.H.) and Biochemistry (S.N., H.K.), Kobe Pharmaceutical University, Kobe, Japan.

Correspondence to: Noriaki Emoto, MD, PhD, Division of Cardiovascular Medicine, Department of Internal Medicine, Kobe University Graduate School of Medicine, 7-5-1 Kusunoki-cho, Chuo-ku, Kobe 650-0017, Japan. E-mail: emoto@med.kobe-u.ac.jp or Hiroshi Kitagawa, PhD, Department of Biochemistry, Kobe Pharmaceutical University, 4-19-1 Motoyamakita-machi, Higashinada-ku, Kobe 658-8558, Japan. E-mail: kitagawa@kobepharma-u.ac.jp

Received July 4, 2013; accepted August 6, 2013.

which regulate the vascular calcification process.[15–17] Extracellular matrix (ECM) components that provide a unique environment for hydroxyapatite mineralization in bone formation[18,19] are considered important factors in the regulation of the progression of vascular calcification. Some ECM molecules such as fibronectin and collagen I induce the in vitro calcification of vascular cells, whereas other molecules such as collagen IV inhibit this process.[20] Accumulation of proteoglycans, another ECM component, in intimal and medial calcification is associated with atherosclerotic plaques as well as calcified nodules in the aortic valve, suggesting that proteoglycans are involved in the development of vascular calcification.[21–23]

Heparan sulfate (HS) and chondroitin sulfate (CS) are glycosaminoglycan chains expressed at the cell surface and in the ECM that modulate various aspects of physiological and pathological conditions.[24–26] These molecules are composed of repeated disaccharide units of *N*-acetylated hexosamine and hexuronic acid that covalently bind to the core protein of proteoglycans through a tetrasaccharide linkage. Sulfation of *N*-acetylated hexosamine and hexuronic acid provides negative charges that enable the binding of ligands.[25–28] The ubiquitous expression of these molecules in various tissues, particularly blood vessels, suggests a contribution to vascular development as well as the progression of vascular diseases.[29–31] Given their roles in osteogenesis,[32–36] glycosaminoglycans may contribute to the osteoblastic differentiation of VSMCs during vascular calcification. However, few studies have addressed the role of glycosaminoglycan modification in the progression of vascular calcification in CKD.

To evaluate the role of glycosaminoglycans in aortic calcification, we used exostosin-like glycosyltransferase 2 deficient (*EXTL2* KO) mice, which overexpress glycosaminoglycans.[37] The mice were subjected to 5/6 subtotal nephrectomy and administered a high-phosphate diet to induce CKD. In this study, we also demonstrated the involvement of glycosaminoglycans in vascular calcification through ex vivo and in vitro studies using aortic rings and VSMCs of *EXTL2* KO mice, respectively. Our study provides evidence that increased glycosaminoglycan expression in murine aortas in CKD augments aortic calcification. In addition, deletion of glycosaminoglycans in VSMCs effectively attenuates in vitro calcification.

Materials and Methods

Animal Studies

The Animal Research and Ethics Committee of Kobe Pharmaceutical University, Kobe, Japan, approved all our animal procedures. In this study, we used *EXTL2* KO mice (n=23) and their wild-type (WT) littermates (n=25) that were previously generated.[37] Both strains were maintained on a C57BL/6 genetic background. Male mice aged 8 to 10 weeks were anesthetized with sodium pentobarbital and subjected to 5/6 subtotal nephrectomy with a 2-step surgical procedure, as described previously (*EXTL2* KO n=15; *EXTL2* WT mice n=16).[38] Sham-operated mice were used as controls (*EXTL2* KO mice n=8; *EXTL2* WT mice n=9). After completion of the 5/6 subtotal nephrectomy, mice received a high-phosphate diet containing 1.5% phosphate (called the CKD groups). Sham-operated groups received a normal-phosphate diet containing 0.5% phosphate (called the control groups) (MF high phosphate diet and MF normal diet; Oriental Yeast Co Ltd). Mice were killed after 8 weeks of diet administration.

Systemic Parameters

Mouse body weight was measured before and at the end of the experiment. Systemic blood pressure was determined by use of a tail-cuff system (Softron) after an acclimatization procedure in conscious mice and with the measurement repeated 10 times for each mouse. With the use of metabolic cages 1 day before the mice were killed, urine was collected. At the end of experiment, blood was taken via cardiac puncture. Blood urea nitrogen and serum phosphate were analyzed by using the urease–glutamate dehydrogenase method and the enzymatic fluorimetric assay for glucose-6-phosphate, respectively. Serum and urine creatinine levels were measured by using an enzymatic assay (Nescoat VLII CRE kit; Alfresa Pharma Corp). The glomerular filtration rate was estimated by measuring the mouse creatinine clearance. Aortic tissue was prepared for calcium measurement, RNA, and histological examinations. Thoracic aorta was used for histology samples, and abdominal aorta was used for calcium and RNA measurement.

In Vitro and Ex Vivo Calcification

Mouse VSMCs were isolated from aorta of control animals (3 mice for each genotype), as previously described.[39] Briefly, aorta was isolated and dissected from the fibrous and lipid tissue in the surrounding area. In the sterile culture medium, aorta was cut into small pieces approximately 1 to 2 mm, and then incubated with type 2 collagenase at 37°C for 6 hours. VSMCs were detached from the tissue by flicking gently, transferred and incubated in 48-well culture dishes, and then left undisturbed for 5 days. Cells with passage numbers 3 to 10 were used for experiment. Cells were culture with high-glucose DMEM (Wako) containing 15% FBS (Biowest), 1% (v/v) penicillin/streptomycin/amphotericin B (Wako), 1 mmol/L sodium pyruvate (Gibco Invitrogen Corp) until 90% to 100% confluence is reached and then treated with high-phosphate medium (inorganic phosphate 3 mmol/L) or normal medium (inorganic phosphate 0.9 mmol/L) as the

normal control for 6 days. Medium was changed every other day. Heparitinase (EC 4.2.2.8, 10 mIU/mL) and chondroitinase ABC from *Proteus vulgaris* (EC 4.2.2.4, 20 mIU/mL) were added to remove HS and CS from the cell surface of VSMCs. Three separated wells were used for each group of treatment. For ex vivo calcification, the dissected thoracic aorta was cut into small rings with a length of approximately 4 to 5 mm and cultured with a normal- or high-phosphate medium for 6 days. Four aortas from 4 different control mice were used for each treatment group.

Calcium Quantification

Aortic and cellular calcium were extracted in the 200 μL of HCl 0.6 mol/L at 4°C for 24 hours and transferred into new tube for calcium quantification. Aortic, cellular, and serum calcium levels were determined by the use of o-Cresophtalein Complexone (Sigma-Aldrich) and commercial detection reagents, according to the manufacturer's protocol. Protein was extracted from aortic samples and cells through incubation with 10% NaOH and 1% SDS and then subjected to protein concentration measurement. The aortic calcium content (μg) was standardized using aortic dry weight (mg). In vitro and ex vivo calcium amounts (μg) were standardized based on the protein content (mg).

Quantitative Real-Time PCR

Messenger RNA was extracted by use of TRIzole reagent (Gibco Invitrogen). The extracted RNA was digested with RQ1 RNase-free DNase and stop solution (Promega) for 30 minutes at 37°C and 10 minutes at 65°C, respectively. Reverse-transcriptase PCR was performed by using Moloney murine leukemia virus reverse transcriptase (Gibco Invitrogen) with random primers (Takara Bio Inc). Quantitative real-time PCR was performed using Fast Start DNA Master plus SYBR Green I and a LightCycler 1.5 (Roche Applied Science) according to the manufacturer's procedures. The primers are for mouse matrix gla protein: forward primer, ccg aga cac cat gaa gag c, and reverse primer, gat tcg tag cac agg gttg; for mouse osteopontin: forward primer, ccc ggt gaa agt gac tga t, and reverse primer, ttc ttc aga gga cac agc att c; for mouse bone morphogenetic protein 2 (BMP2): forward primer, atg taa tca gaa gaa ata tcg ggt, and reverse primer, gga ctt gaa ctt gtg aac ttt aac; for mouse BMP receptor type Ia (BMPRIa): forward primer, cca tta tag aag aag atg atc agg g, and reverse primer, ctg caa ata ctg gtt gca c; for mouse BMP receptor type II (BMPRII): forward primer, agg cag cca aca tag tg, and reverse primer: agg cag cca aca tag tg; and for mouse glyceraldehyde-3-phosphate dehydrogenase (GAPDH): forward primer, cat ctg agg gcc cac tg, and reverse primer, gag gcc atg tag gcc atg a.

Immunohistochemistry and Histology

Aortic tissue was fixed in the 4% paraformaldehyde in PBS (v/v) at 4°C for overnight. The fixated aorta was subjected to paraffin or frozen block preparation. Then, 4-μm slides were used for hematoxylin-eosin staining and immunohistochemistry. After performing antigen retrieval step using citrate buffer, the samples were permeabilized using 0.05% Triton X-100 in PBS (v/v) and blocked in the 5% BSA in PBS (v/v). The primary antibodies are anti-HS antibody, HepSS-1, anti-CS antibody, 3B3, 1:100 (Seikagaku Biobusiness Corporation, Tokyo, Japan), antiphosphorylated (p)-smad1/5/8 antibody 1:100, anti–smooth muscle–22α antibody 1:100 (Cell Signaling Technologies), anti–α–smooth muscle actin–FITC antibody 1:100 (Sigma Aldrich Corp), anti–runt-related transcription factor 2 antibody, 1:100 (Santa Cruz Biotechnology). After an adequate washing step, the samples sections were incubated with appropriate secondary antibodies. Images were captured with an LSM 710 laser-scanning confocal microscope using a $\times$20 objective. Overt matrix mineralization and calcium deposition in the mouse aorta and VSMCs were detected by using Von Kossa staining and alizarin red, respectively.

Glycoaminoglycan Fluorescent Labeling and Immunocytochemistry

Mouse VSMCs were fixed in 4% Paraformaldehyde (PFA) in PBS (v/v). Fixated cells were permeabilized in 0.05% Triton X-100 in PBS (v/v) before blocking with 5% BSA in PBS (v/v). HepSS-1 and CS56 primary antibodies (Sigma Aldrich) were used for labeling the HS and CS, respectively. To observe apoptosis process, anti–caspase 3 antibody (Santa Cruz Biotechnology) was used. After incubation with the appropriate secondary antibodies, images were captured using an LSM 710 laser-scanning confocal microscope with a $\times$10 objective.

Proliferation and Migration Assays

To examine the proliferation activity of VSMCs, the cell proliferation reagent WST-1 was used according to the manufacturer's protocol. Briefly, VSMCs (4×10^3 cells/well) were culture to 50% confluence. The cells were treated with medium containing 15% FBS. The chondroitinase ABC and heparitinase were added to the well of enzyme-treated group. Cells with free serum medium were used as a control. After a 24-hour incubation, 10 μL of WST-1 reagent was added to each well, and the cells were reincubated for an additional 2 hours. The color intensity was read at 450 nm (reference wavelength 655 nm). To measure migration activity, we used scratch wound assay as described previously.[40] VSMCs were seeded into 6-well dishes. Confluent monolayers were scraped through the middle of the dish by using a modified

100-μL tip. After wounding, monolayers were immediately washed with DMEM and incubated with 15% FBS. Heparitinase and chondroitinase ABC were added in the enzyme–treated group. After 48 hours, wound closure area from the wound edge was quantified.

BMP2 Accumulation Assay in Aortic Tissue

Recombinant human BMP2 (rhBMP2) (R&D Systems) (1 μg/mL) was preincubated with goat antipolyclonal BMP2 (Santa Cruz Biotechnology) (2 μg/mL) at 37°C for 30 minutes. Fixed aortic tissue was incubated with the ligand–antibody complex at 4°C for 30 minutes. Following incubation, the aortic tissues were washed with PBS and blocked using 5% BSA at room temperature for 30 minutes. The aortic samples were incubated in donkey antigoat Alexa Fluor 488–conjugated secondary antibody. Fluorescence was visualized using an LSM 710 laser-scanning confocal microscope with a ×20 objective.

Disaccharide Composition Analysis in Aortic Tissue

The aorta was harvested from 8-week-old male mice (3 mice for each genotype), homogenized in cold acetone, and evaporated overnight. The resulting dry powder was digested by actinase E at 55°C for 24 hours. The digested sample was resuspended in 5% trichloroacetic acid and centrifuged, and the supernatant was extracted using diethyl ether. The aqueous phase was neutralized and precipitated using 80% ethanol. The precipitate was dissolved in pyridine acetate buffer and subjected to filtration on a PD-10 column (GE Healthcare). The flow-through products were evaporated, and the dried samples were digested using a mixture of heparitinase (EC 4.2.2.8, 1 mIU) and heparinase (EC 4.2.2.7, 1 mIU) from *Flavobacterium heparinum* or chondroitinase ABC from *P. vulgaris* (EC 4.2.2.4, 10 mIU) at 37°C for 4 hours. The digested glycosaminoglycans were derivatized using the fluorophore 2-aminobenzamide and then analyzed by using a high-performance liquid chromatography–SLC-10A system (Shimadzu) on a PA-03 column (YMC) as reported previously.[41]

Statistical Analysis

Results are presented as the mean±SEM. The data distribution was tested using Kolmogorov-Smirnov test. Normally distributed variables were analyzed using ANOVA followed with the unpaired Student *t* test. Variables not normally distributed were analyzed using nonparametric analysis with Kruskal-Wallis followed by Mann-Whitney *U* test. All analyses were performed using GraphPad Prism software. Differences were considered significant when $P<0.05$.

Results

Augmented Glycosaminoglycan Chains (HS and CS) in Aortas of *EXTL2* KO Mice

The disaccharide content of glycosaminoglycan chains (HS and CS) in the aortas of *EXTL2* KO mice was higher than that in the aortas of WT mice (Tables 1 and 2). We also examined disaccharide composition in those mice and found that the 6-sulfation pattern composition of CS in *EXTL2* KO mice is higher compared with that in *EXTL2* WT mice.

Table 1. Disaccharide Composition of HS From Aorta of *EXTL2* KO or WT Mice

Composition	Aorta, pmol/mg (mol%)	
	EXTL2 KO	WT
ΔDiHS-0S	464.6±70.7 (38.4)	239.8±70.7 (38.4)
ΔDiHS-6S	35.3±13.7 (3.1)	28.5±13.4 (4.6)
ΔDiHS-NS	535.2±67.0 (46.4)	266.5±43.1 (42.7)
ΔDiHS-diS_1	21.9±7.2 (1.9)	12.7±4.6 (2.0)
ΔDiHS-diS_2	82.2±6.6 (7.1)	69.2±16.9 (11.1)
ΔDiHS-TriS	14.5±3.5 (1.3)	7.5±3.8 (1.2)
Total	1153.8±209.2 (100)*	624.4±139.6 (100)

Aorta of *EXTL2* KO mice contains higher HS amounts than those of WT mice. Disaccharide composition of HS from aorta of 8-week-old male mice. Data are shown as pmol of disaccharide per mg of acetone powder of aorta, the mean±SEM, and percentage from total amount of 3 independent experiments. Di-diS_2 indicates ΔHexUA (2S) α1-4GlcNS; ΔDiHS-0S, ΔHexUA α1-4GlcNAc; ΔDiHS-6S, ΔHexUA α1-4GlcNAc(6S); ΔDiHS-diS_1, ΔHexUA α1-4Glc(NS,6S); ΔDiHS-NS, ΔHexUA α1-4GlcNS; ΔDi-triS, ΔHexUA (2S) α1-4Glc(NS,6S); *EXTL2* KO, *exostosin-like glycosyltransferase 2* knockout; HS, heparan sulfate; WT, wild-type.
*$P<0.05$ vs WT mice by the unpaired Student *t* test.

Table 2. Disaccharide Composition of CS From Aorta of *EXTL2* KO and WT Mice

Composition	Aorta, pmol/mg (mol%)	
	EXTL2 KO	WT
ΔDiCS-0S	138.2±57.8 (18.7)	123.5±50.1 (25.4)
ΔDiCS-6S	257.9±33.7 (34.8)*	121.5±26.8 (25.0)
ΔDiCS-4S	332.2±112.1 (44.8)	234.3±70.0 (48.2)
ΔDiCS-diSD	12.4±2.9 (1.7)	6.4±1.9 (1.3)
ΔDiCS-diSE	ND	ND
ΔDiCS-TriS	ND	ND
Total	740±145.5 (100)*	485.7±145.4 (100)

Aorta of *EXTL2* KO mice contains higher CS amounts than those of WT mice. Disaccharide composition of CS from aorta of 8-week-old male mice. Data are shown as pmol of disaccharide per mg of acetone powder of aorta, the mean±SEM, and percentage from total amount of 3 independent experiments. ΔDi-0S indicates ΔHexUA α1-3GalNAc; ΔDi-4S, ΔHexUA α1-3GalNAc(4S); ΔDi-6S, ΔHexUA α1-3GalNAc (6S); ΔDi-diSD, ΔHexUA(2S) α1-3GalNAc(6S); ΔDi-diSE, ΔHexUA α1-3GalNAc(4S,6S); ΔDi-triS, ΔHexUA(2S) α1-3GalNAc(4S,6S); CS, chondroitin sulfate; *EXTL2* KO, *exostosin-like glycosyltransferase 2* knockout; ND, not detected; WT, wild-type.
*$P<0.05$ vs WT mice by the unpaired Student *t* test.

Equal Development of CKD in *EXTL2* KO and WT Mice Following 5/6 Subtotal Nephrectomy and High-Phosphate Diet Administration

To determine the presence of CKD, the blood urea nitrogen and glomerular filtration rate were measured in *EXTL2* KO and WT mice. In both CKD groups, the kidney function was markedly reduced, as demonstrated by a higher blood urea nitrogen and a lower GFR (Figure 1A and 1B). No significant difference between the 2 genotypes was observed under normal conditions. As expected, the high-phosphate diet in the CKD group induced high serum phosphate levels, with no effect on serum calcium levels; thus, the serum Ca×P product was increased in both genotypes (Figure 1C through 1E). The mouse body weight decreased in all CKD groups, and a lower body weight was detected in *EXTL2* KO mice (Figure 2A). Systolic blood pressure levels were elevated in *EXTL2* KO mice with CKD (Figure 2B).

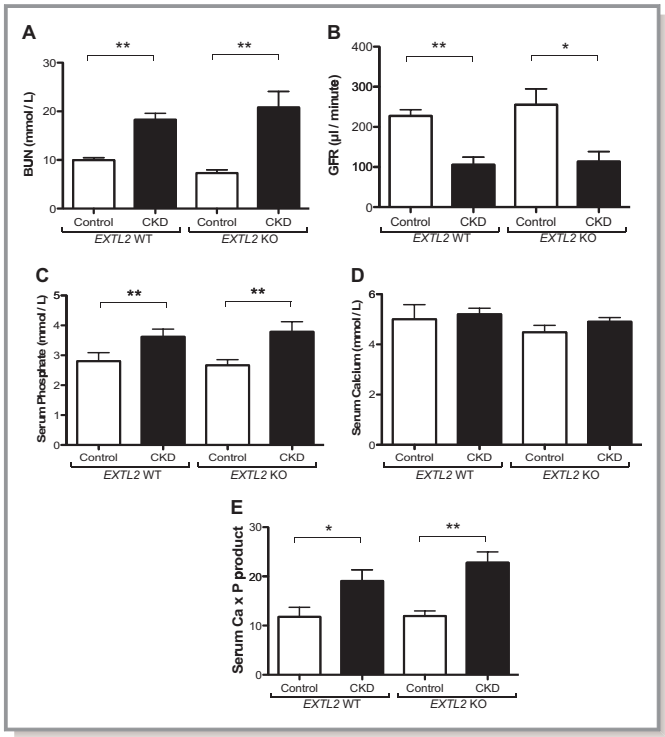

Figure 1. Development of CKD that represented by serum chemistry was independent from genotype of all groups. A, All mice under CKD groups have higher blood urea nitrogen (BUN), reaching 2-fold differences compared with control groups. B, In addition, both *EXTL2* KO and WT mice in the CKD groups have a lower glomerular filtration rate (GFR): approximately 50% less than in the control groups. C, Mice with CKD have significantly higher serum phosphate levels than control groups. D, However, serum calcium concentration was determined to be at the same level in all comparable groups. E, The product of serum Ca×P was higher in the CKD groups than in the control groups. Data are shown as mean±SEM (n=3 to 6), **P*<0.05, ***P*<0.01; BUN, serum phosphate, and serum calcium by the unpaired Student *t* test and GFR and serum Ca×P product by the Mann-Whitney *U* test. CKD indicates chronic kidney disease; *EXTL2* KO, *exostosin-like glycosyltransferase 2* knockout; WT, wild-type.

Increased Aortic Calcification in Aortas of *EXTL2* KO Mice With CKD

Reduced renal function and high phosphate levels contribute to the development of aortic calcification. We determined the aortic calcification by using a qualitative and a quantitative method: Von Kossa staining and aortic calcium content measurement, respectively. We used Von Kossa staining to show overt calcification. We found that Von Kossa staining was positive in only 5 of the 15 *EXTL2* KO mice with CKD, which mean 33% of the mice in this group showed overt calcification (Figure 3A through 3H). Calcification was mainly visible in the media layer of aorta, within and surrounding the elastic fibers; this layer predominantly consists of VSMCs. All other experimental groups did not show overt signs of calcification. Furthermore, to measure the extent of aortic calcification, we measured the calcium content in the aorta. Even though, not all *EXTL2* KO mice under CKD showed overt calcification; the average of the calcium content in this group is the highest among all groups (Figure 3M). To confirm that HS and CS chains are important for aortic calcification, isolated aortic rings from control mice of both genotypes were cultured in normal- or high-phosphate medium. As shown in Figure 3N, although the high-phosphate medium elevated the calcium deposition in both genotypes, the aorta of *EXTL2* KO mice demonstrated significantly higher calcium deposition than that of WT mice.

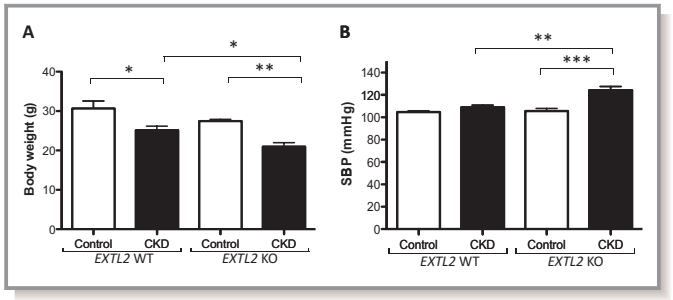

Figure 2. Chronic kidney disease (CKD) influenced body weight and blood pressure after 2 months of treatment. A, After 2 months of treatment, marked weight loss was found in all CKD groups. Also, *EXTL2* KO mice have a lower body weight than WT mice. B, CKD-induced *EXTL2* KO mice have remarkably higher systolic blood pressure (SBP) than the control and WT mice. Data are shown as mean±SEM (n=7 to 9), **P*<0.05, ***P*<0.01, ****P*<0.005 by the unpaired Student *t* test. *EXTL2* KO indicates *exostosin-like glycosyltransferase 2* knockout; WT, wild-type.

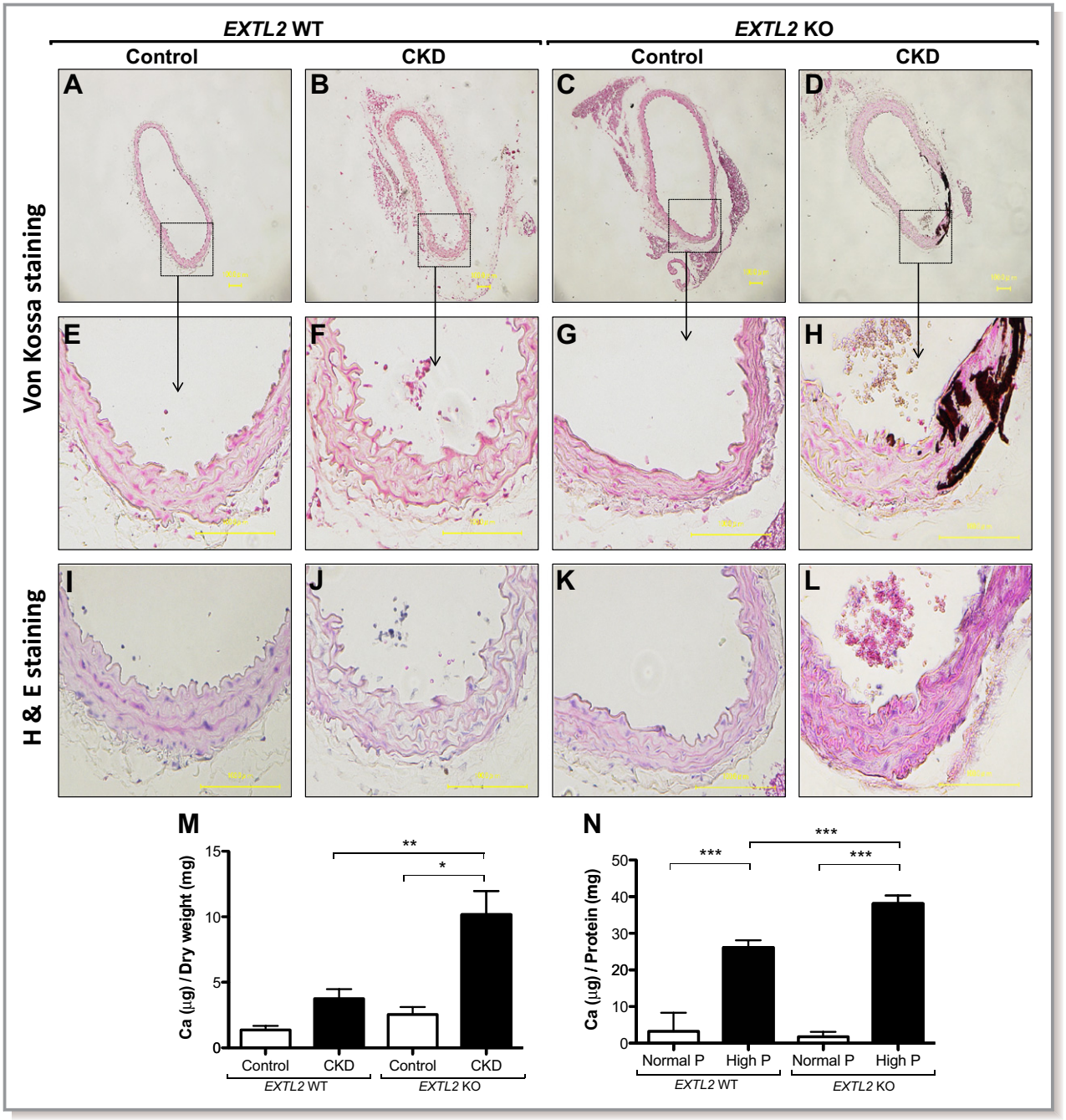

Figure 3. Deleting the *EXTL2* gene aggravated aortic calcification under CKD. A through H, Calcium deposition (black) visualized by Von Kossa staining was predominantly in the aortic media. I through L, Aortic structure was shown by the use of hematoxylin and eosin (H&E) staining. M, Quantification of calcium content in the mice aorta has shown that *EXTL2* KO mice under CKD developed more calcium deposition than WT mice (control group, n=5 to 6; CKD group, n=15 to 16). Data are shown as mean±SEM, **P*<0.05, ***P*<0.01 by Mann-Whitney *U* test. N, Calcium deposition quantification in aortic culture of *EXTL2* KO and WT mice after 6 days of phosphate treatment (n=5 separated mice). Data are shown as mean±SEM, ****P*<0.005 by the unpaired Student *t* test. CKD indicates chronic kidney disease; *EXTL2* KO, *exostosin-like glycosyltransferase 2* knockout; WT, wild-type.

Alterations in Bone Matrix Components and VSMC Markers in the Calcified Aorta of *EXTL2* KO Mice

Immunostaining revealed a high expression of the osteoblastic differentiation markers runt-related transcription factor 2 (Figure 4E through 4M) and type Ia collagen (Figure 5E through 5M) in the calcified aorta of *EXTL2* KO mice but little or no expression in the other groups. Concomitant with the calcium deposition in the aorta, the mRNA level of matrix gla protein increased in the *EXTL2* KO mice with calcified aortas compared with that in WT mice

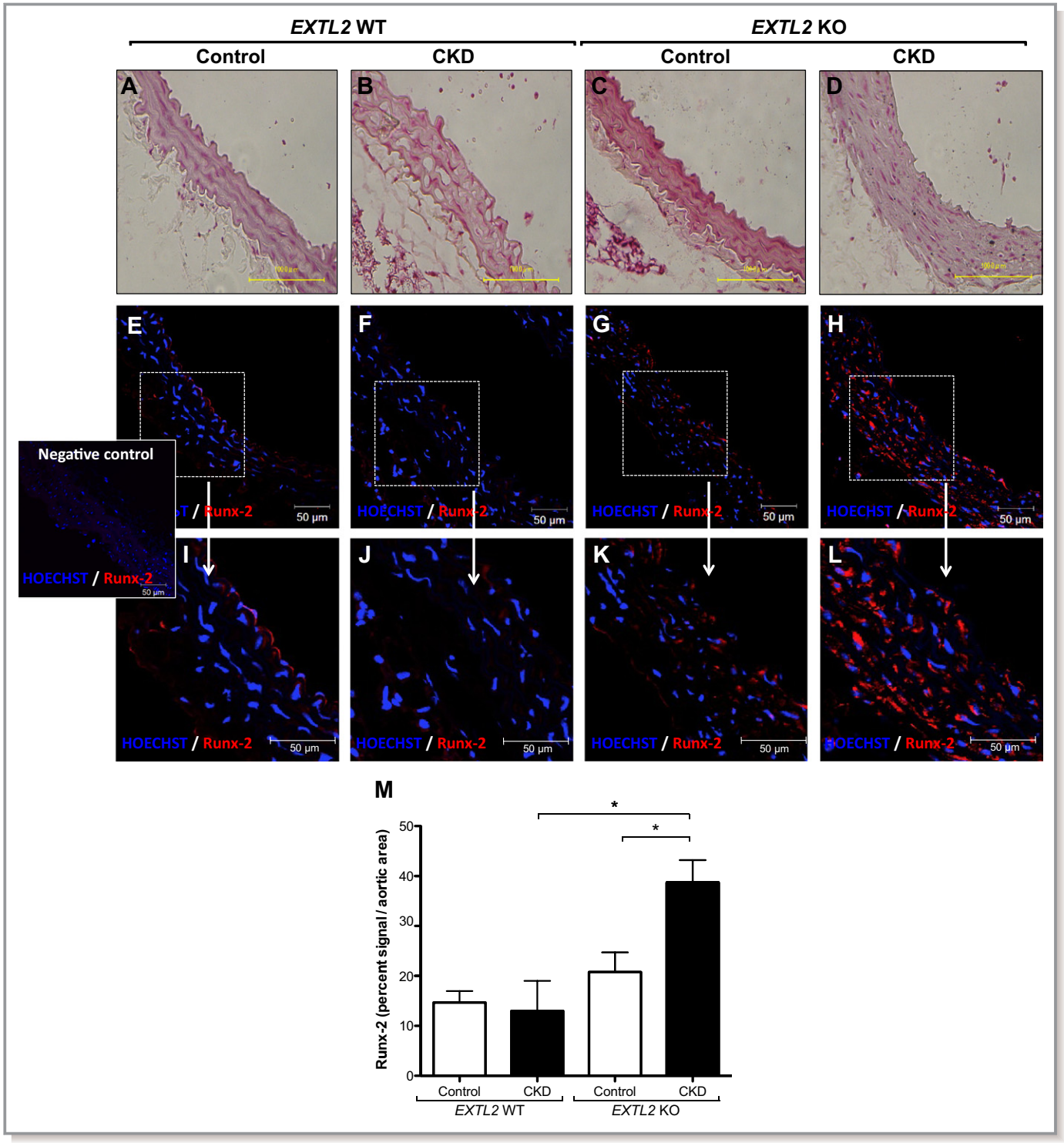

Figure 4. Enhancement of Runx2 in *EXTL2* KO mice aorta. A through D, Serial section of each group was detected by Von Kossa staining. E through L, Runx2, which is associated with osteoblastic differentiation, was enhanced in the calcified aorta of *EXTL2* KO mice. M, Quantification result of Runx2 signal per aortic area. Data are shown as mean±SEM (n=6), **P*<0.05 by Mann-Whitney *U* test. *EXTL2* KO indicates *exostosin-like glycosyltransferase 2* knockout; Runx2, runt-related transcription factor 2.

with CKD and the other control groups (Figure 6A). Similarly, the osteopontin mRNA level was up-regulated in the calcified aorta of *EXTL2* KO mice (Figure 6B). In addition, calcified aorta of *EXTL2* KO mice demonstrated a loss of VSMC markers such as smooth muscle–22α and α–smooth muscle actin (Figure 7).

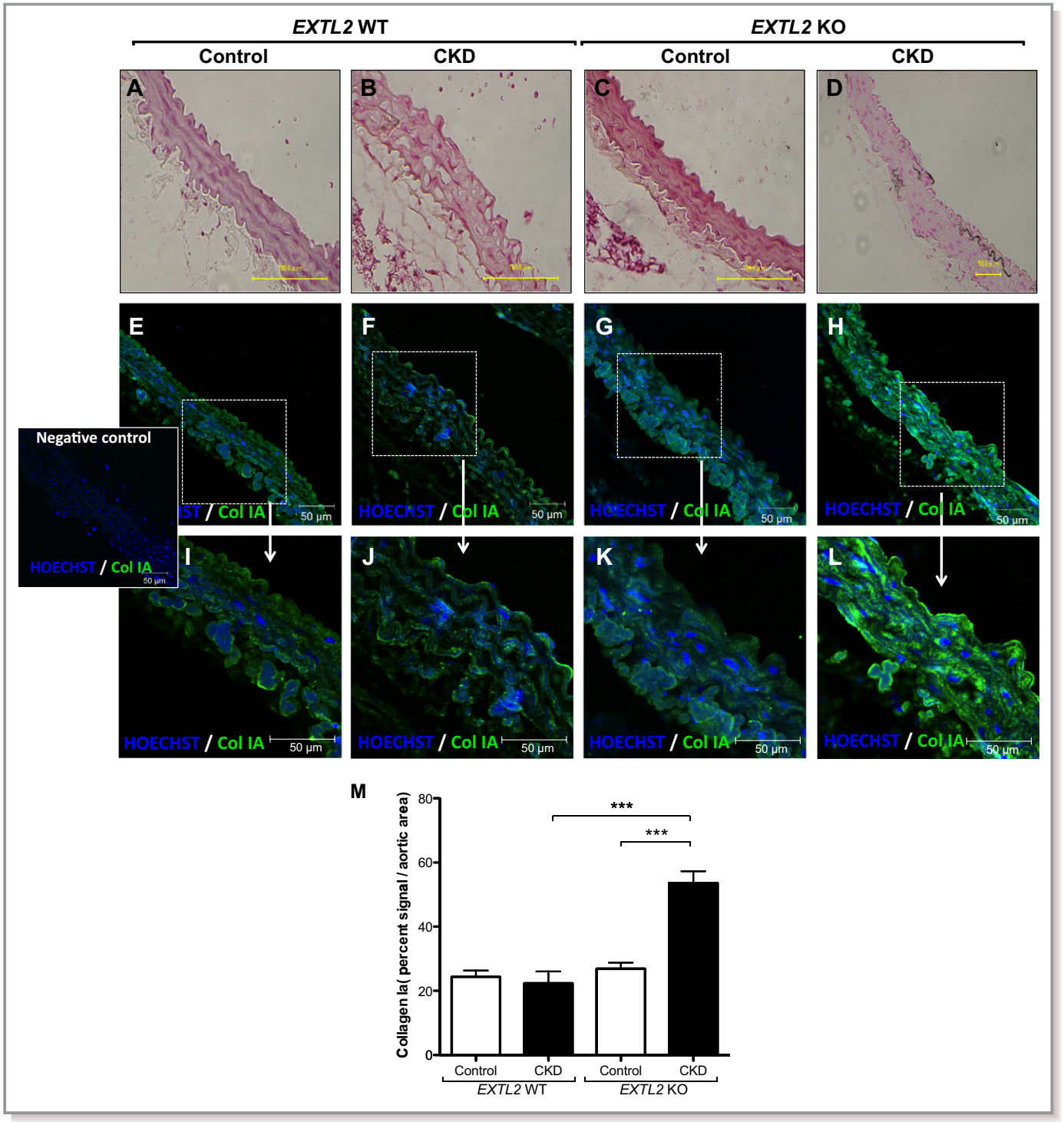

Figure 5. Augmentation of collagen Ia in calcified aorta of *EXTL2* KO mice. A through D, Serial section of each group was detected by Von Kossa staining. E through L, Collagen Ia was up-regulated in the calcified aorta of *EXTL2* KO mice. M, Quantification result of collagen Ia signal in aortic area. Data are shown as mean±SEM (n=6), ***$P<0.005$ by the unpaired Student *t* test. Col Ia indicates collagen Ia; *EXTL2* KO, *exostosin-like glycosyltransferase 2* knockout.

CKD Increases HS and CS Levels in Calcified and Noncalcified Aortas

The accumulation of ECM components in calcified lesions is considered to stimulate subsequent vascular calcification. In the present study, HS and CS levels were much higher in the calcified aortas of CKD-induced *EXTL2* KO mice than in the aortas of control *EXTL2* KO mice, which already showed an up-regulation of HS and CS in their aortas. HS and CS levels

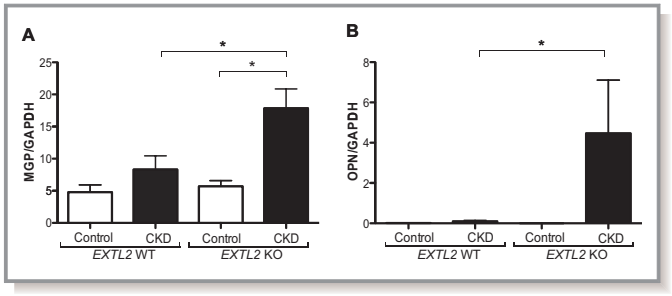

Figure 6. Enhancement of bone matrix components in *EXTL2* KO mice aorta. A and B, Quantitative real-time PCR results show an up-regulation of MGP and OPN in calcified aorta. Data are shown as mean±SEM (n=4 to 6), **P*<0.05 by Mann-Whitney *U* test. *EXTL2* KO indicates *exostosin-like glycosyltransferase 2* knockout; GAPDH, glyceraldehyde-3-phosphate dehydrogenase; MGP, matrix gla protein; OPN, osteopontin; PCR, polymerase chain reaction.

were also increased in the noncalcified aortas of CKD-induced WT mice (Figure 8).

Attenuation of HS or CS Expression Decreases Calcium Deposition in VSMCs Cultured in High-Phosphate Conditions

Heparitinase and chondroitinase treatment effectively reduced HS and CS expression on the cell surface of VSMCs, respectively (Figure 9). These treatments have no significant effects on proliferation, migration, or apoptosis activity in treated VSMCs (Figure 10). Under high-phosphate treatment, alizarin red staining and calcium quantification revealed matrix mineralization in mouse VSMCs (Figure 11). In support of the in vivo results, *EXTL2* KO VSMCs that overexpressed HS and CS demonstrated higher calcium deposition (33% increase) under the high-phosphate condition than those from WT mice. To investigate which glycosaminoglycan contributed to vascular calcification, removal of HS or CS via enzymatic digestion was performed in vitro in high-phosphate mouse VSMCs. Heparitinase treatment effectively decreased the amount of alizarin red staining and the calcium level in high-phosphate–induced mouse VSMCs. Furthermore, treatment with chondroitinase also markedly reduced matrix mineralization and calcium deposition in high-phosphate–containing *EXTL2* KO and WT mouse VSMCs.

Up-regulation of BMP2 Signaling in the Calcified Aorta

Many studies have shown that BMP2 signaling positively contributes to osteoblastic differentiation of VSMCs during vascular calcification. In the present study, we observed that BMP2 mRNA was increased in both CKD groups. No difference was observed in the expression of BMPR Ia and BMPR II. The p-Smad1/5/8 expression downstream of BMP signaling was detected clearly only in the calcified aortas of *EXTL2* KO mice (Figure 12). In addition, extracellular BMP2 accumulated to a greater extent in the calcified aorta than in the WT aorta (Figure 13).

Discussion

In this study, we demonstrate that the overexpression of HS and CS contributes to vascular calcification in CKD in vivo. We also confirmed the involvement of HS and CS in vascular calcification through ex vivo and in vitro studies. Under high-phosphate conditions, the calcium deposition was increased in aortic tissue samples and aortic VSMCs derived from *EXTL2* KO mice compared with those from WT mice. Furthermore, deletion of HS or CS in mouse VSMCs decreased the amount of calcium deposition. These findings suggest that HS and CS enhanced the vascular calcification progression under high-phosphate conditions.

To evaluate the involvement of HS and CS in vascular calcification, we used *EXTL2* KO mice, which show elevated HS and CS expression. *EXTL2* is an enzyme involved in HS and CS biosynthesis; in particular, it has transferase activity, and mediates the transfer of the first *N*-acetylglucosamine via an α1,4 linkage to a phosphorylated tetrasaccharide core region, which results in the termination of HS and CS.[25,37,42] Deletion of *EXTL2* in mice disturbs this process and permits the accumulation of HS and CS in vivo. *EXTL2* KO mice show an increased HS and CS expression in the liver, brain, and embryonic fibroblasts.[37] In the present study, we also observed high HS and CS expression in the aorta of these mice. HS and CS were clearly expressed in the aorta, particularly in the sub-endothelial and medial layers. It is likely that the lack of *EXTL2* in mice did not affect their growth process, as they grew normally and had normal blood pressure under physiological conditions. In addition, there is no study reported about the role of *EXTL2* and other *EXT*'s families beyond the regulation of glycosaminoglycan biosynthesis. Therefore, we considered that the excess glycosaminoglycan expression in the *EXTL2* KO mouse might contribute during pathological conditions particularly to vascular calcification development. In support of our results, the current report by Nadanaka et al[43] showed the important role of *EXTL2*-mediated glycosaminoglycan synthesis in regenerating process during liver injury. Regarding our hypothesis that glycosaminoglycan overproduction might have deleterious effects during vascular calcification, we used mice of the C7BL/6J strain that are relatively resistant to vascular calcification,[44] which allowed us to evaluate the role of HS and CS in enhancing vascular calcification.

The severity of CKD has an important role in the development of vascular calcification. Therefore, we examined

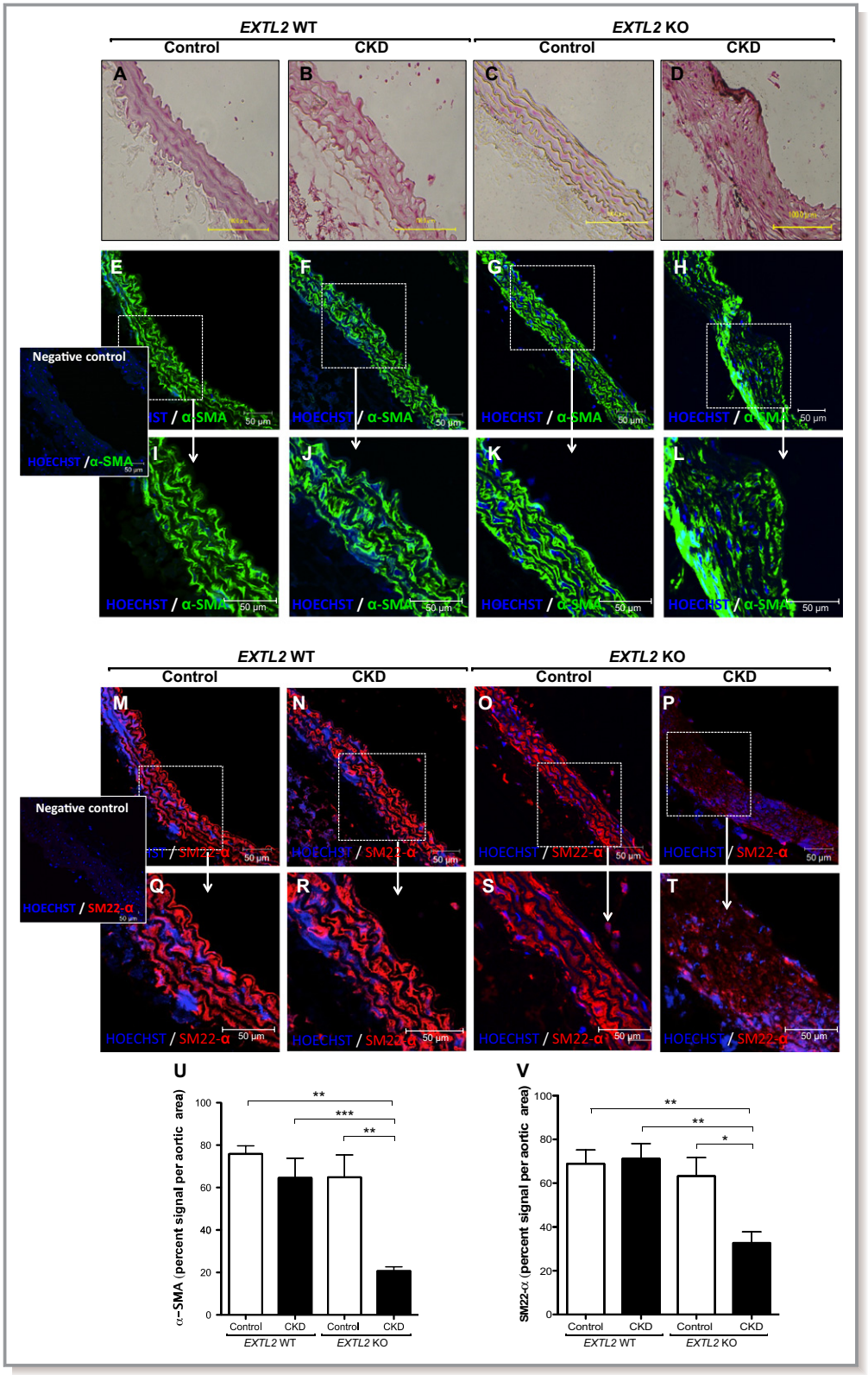

Figure 7. Vascular smooth muscle cell loss in the calcified aorta of *EXTL2* KO mice. A through D, Serial section of each group was detected by the use of Von Kossa staining. α-SMA (E through L) and SM22-α (M through T) as contractile phenotype markers of VSMCs were highly expressed in both control groups and the CKD group of WT mice. However, their expression was attenuated in the calcified aorta of *EXTL2* KO mice under the CKD condition. Quantification result of α-SMA (U) and SM22-α (V) signal in aortic area. Data are shown as mean±SEM (n=6), **P*<0.05, ***P*<0.01, ****P*<0.005 by the unpaired Student *t* test. CKD indicates chronic kidney disease; *EXTL2* KO, *exostosin-like glycosyltransferase 2* knockout; SMA, smooth muscle actin; SM, smooth muscle; VSMC, vascular smooth muscle cell; WT, wild-type.

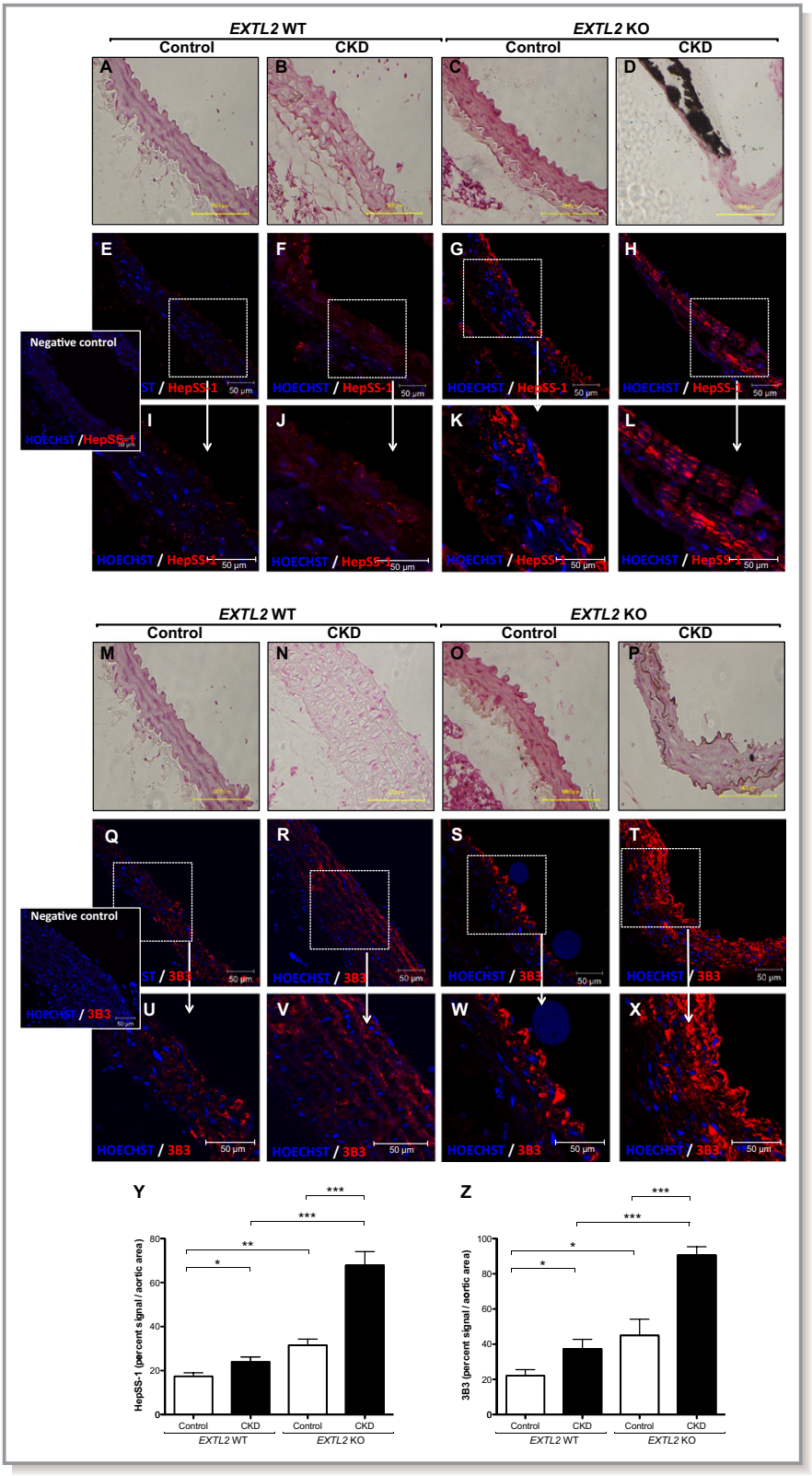

Figure 8. Heparan sulfate (HS) and chondroitin sulfate (CS) signals were increased in CKD treated group. A through D, Serial section of each group was detected by Von Kossa staining. HS and CS expression in mice aorta were detected by HepSS-1 (E through L) and 3B3 (Q through X) antibody, respectively. Their expressions were up-regulated under CKD. HepSS-1 and 3B3 signals were quantified and shown as percentage per aortic area (Y and Z, respectively). Data are shown as mean±SEM (n=6), **P*<0.05, ***P*<0.01, ****P*<0.005 by the unpaired Student *t* test. 3B3 indicates anti-CS antibody; CKD, chronic kidney disease; *EXTL2* KO, *exostosin-like glycosyltransferase 2* knockout; HepSS-1, anti-HS antibody; WT, wild-type.

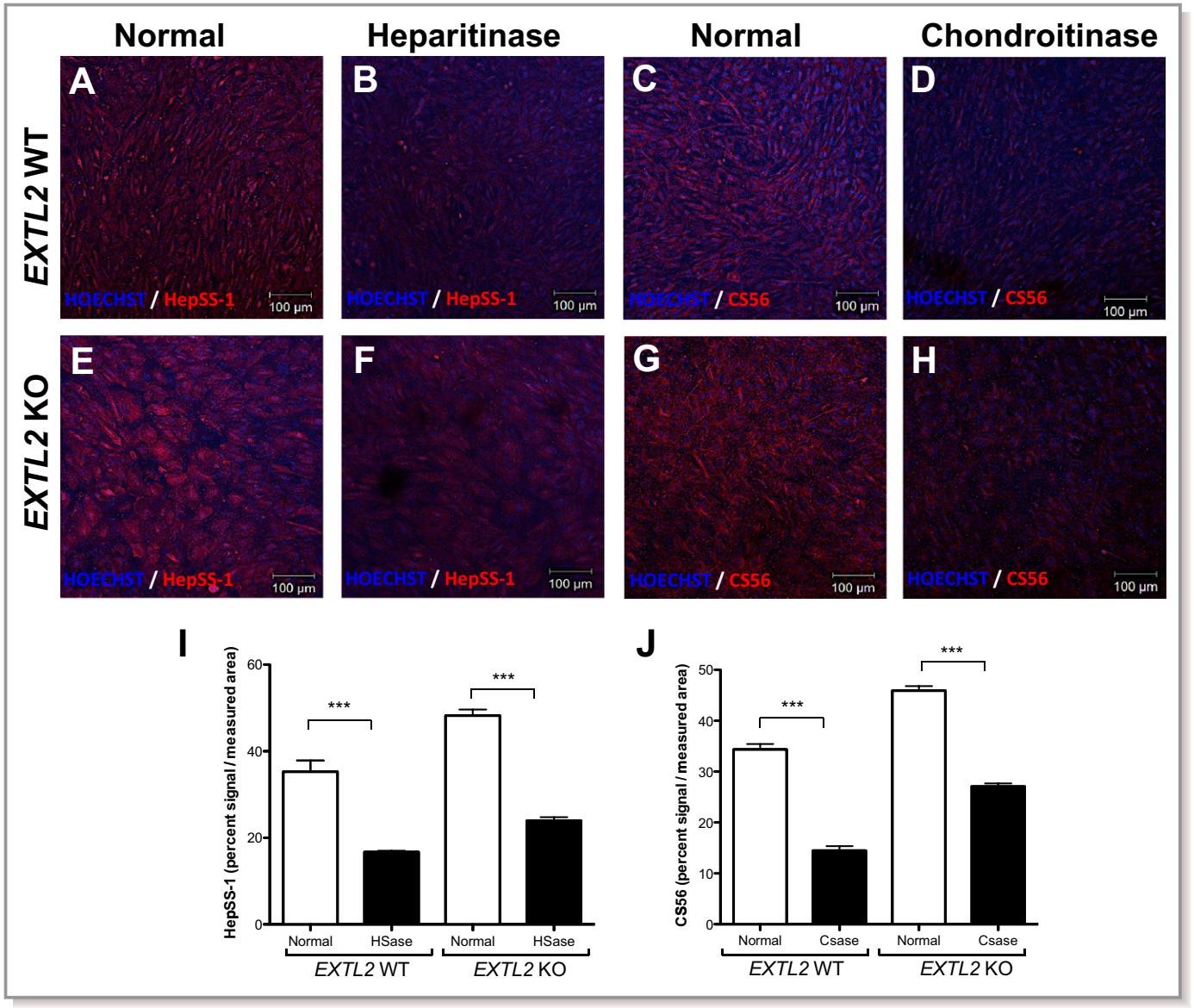

Figure 9. Heparan sulfate (HS) and chondroitin sulfate (CS) expressions were reduced under enzyme treatment. HS (A, B, E, F) and CS (C, D, G, H) expressions were reduced after heparitinase and chondroitinase treatment, respectively. HepSS-1 and CS56 signals were quantified and shown as percentage per measured area (I and J, respectively). Data are shown as mean±SEM (n=6), ***$P<0.005$ by the unpaired Student *t* test. *EXTL2* KO indicates *exostosin-like glycosyltransferase 2* knockout; WT, wild-type.

the kidney function in all comparable mouse groups. However, we observed that kidney functions did not differ between *EXTL2* KO and WT mice, under either normal conditions or following CKD induction. Considering the importance of phosphate in the development of vascular calcification, we also examined the serum phosphate concentration in all treatment groups. We found that the phosphate concentration was not affected by genotypic differences. Systolic blood pressure was initially similar among all the treatment groups. In our study, *EXTL2* KO mice did not develop aortic calcification spontaneously. Interestingly, after 2 months of CKD with high-phosphate conditions, the *EXTL2* KO mice clearly showed more vascular calcification than the WT mice and developed higher systolic blood pressure than the WT mice. We assume that vascular calcification, which is accompanied by increased stiffness and decreased compliance of arteries,[45,46] increased systolic blood pressure. From these results, we suggest that overproduction of glycosaminoglycan in *EXTL2* KO mice enhanced the aortic calcification under CKD with high-phosphate conditions.

To support the in vivo finding that demonstrates the role of glycosaminoglycan in vascular calcification, we also conducted an ex vivo study using aortic rings and an in vitro study using aortic VSCMs isolated from both *EXTL2* KO and WT control group mice. Our ex vivo study showed that aortic ring tissue from *EXTL2* KO mice has a higher calcium deposition

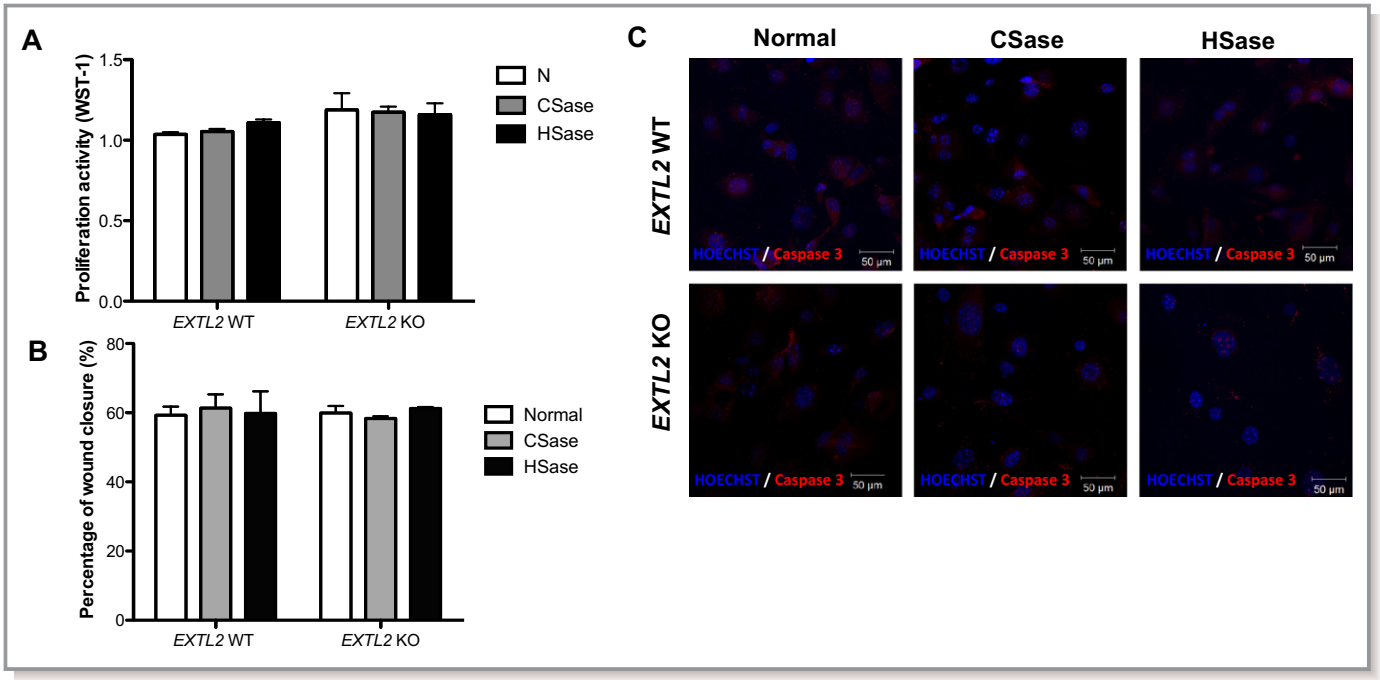

Figure 10. Proliferation, migration, and apoptosis activities are not affected by enzyme treatment. Proliferation (A) and migration (B) activities of both genotype VSMCs were not significantly different and not affected by heparitinase or chondroitinase treatment. C, Caspase 3 expression was at a similar level in all treated groups. Data are shown as mean±SEM (n=3) by Mann-Whitney *U* test. CS indicates chondroitin sulfate; *EXTL2* KO, *exostosin-like glycosyltransferase 2* knockout; HS, heparan sulfate; VSMC, vascular smooth muscle cell; WT, wild-type.

than that from WT mice in the presence of high-phosphate medium. The in vitro study showed that VSMCs of the *EXTL2* KO mice in the presence of high-phosphate medium have a higher calcium deposition than those of the other groups. Furthermore, we showed that the deletion of HS and CS using heparitinase and chondroitinase, respectively, results in lowering the calcium deposition under high-phosphate conditions. These results confirmed that overexpressed glycosaminoglycan might contribute in aortic calcification under high-phosphate conditions.

Previous studies suggested that proteoglycan contributes to the progression of vascular calcification. Decorin, a chondroitin sulfate proteoglycan, was found at sites of calcification within the aortic valve[23] and atherosclerotic plaque of human coronary arteries.[21] Increased decorin expression promotes in vitro calcification of VSMCs.[21] In addition, other chondroitin sulfate proteoglycans, biglycan, and versican were expressed in calcified nodules and areas surrounding calcified lesions in the aortic valve, which suggests that biglycan and versican actively induce and modulate soft tissue mineralization, respectively.[23] However, these studies provide no evidence for the contribution of HS and CS to vascular calcification. Our study suggests that accumulation of HS and CS in the mice aorta contributes to matrix mineralization in the aorta. The negative charges of sulfate residue in HS and CS create ligand-binding sites and modulate their activity. The most well-known growth factor ligand related to osteoblastic differentiation is BMP2. By acting as a coreceptor for BMP2, HS accelerates the formation of a complex between BMP2 and BMP receptors and contributes to enhance BMP2 signaling.[27] HS modulates the distribution of BMP2 on the cell surface, prolongs the half-life of BMP2, and reduces the interaction of BMP2 with its antagonist.[34] In a human study, Koleganova et al observed that BMP2 expression was higher in the aorta of CKD patients than in controls, but no difference was found between calcified and noncalcified aortas.[47] Consistent with this study, we observed a higher level of BMP2 in CKD mice than control mice. However, we did not observe any difference in BMP2 and BMPR receptor expression in either CKD group. Interestingly, p-smad1/5/8 activation was detected higher in the calcified aortas of *EXTL2* KO mice than in the aortas of the other groups. These results suggested that overproduction of HS might mediate the BMP2 binding with BMP receptors and activate the signal transduction. To visualize BMP2 distribution in aortic tissue, we performed BMP2 accumulation assays and found that BMP2 was more abundantly accumulated in calcified aortas than in tissues from other groups. It is likely that high HS and CS levels in CKD contribute to the attachment of BMP2 to BMP receptors and the activation of downstream signaling. Activation of BMP2 signaling has been further shown to affect the phenotypic transition of VSMCs.[48]

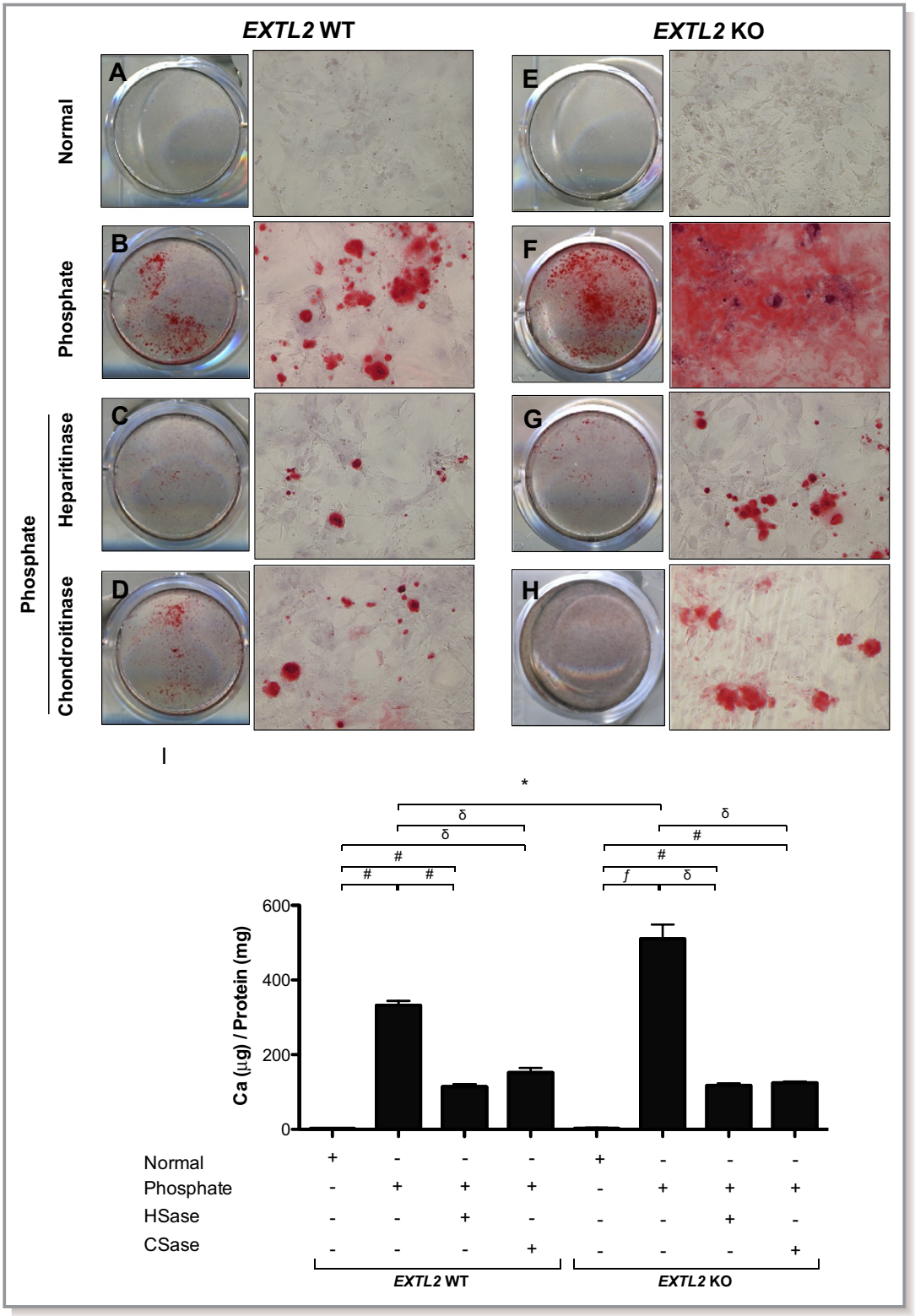

Figure 11. Removal of heparan sulfate (HS) and chondroitin sulfate (CS) cell surface structure ameliorated calcium deposition of high-phosphate–treated VSMCs. A, B, E, F, Alizarin red–positive area was markedly up-regulated in phosphate-treated cells, and an extensive positive area was found in *EXTL2* KO mouse VSMCs. C, G, Removal of HS with use of heparitinase 10 mIU/mL effectively attenuated calcium deposition under high-phosphate conditions. D, H, CS digestion by chondroitinase 20 mIU/mL treatment also decreased the amount of calcium deposition with high-phosphate treatment. I, Calcium deposition was quantified by using the o-Cresophtalein Complexone method in all comparable groups. Data are presented as mean±SEM (n=3), **P*<0.05, δ<0.001, ƒ*P*<0.0005, #*P*<0.0001 by the unpaired Student *t* test. *EXTL2* KO indicates *exostosin-like glycosyltransferase 2* knockout; VSMC, vascular smooth muscle cell; WT, wild-type.

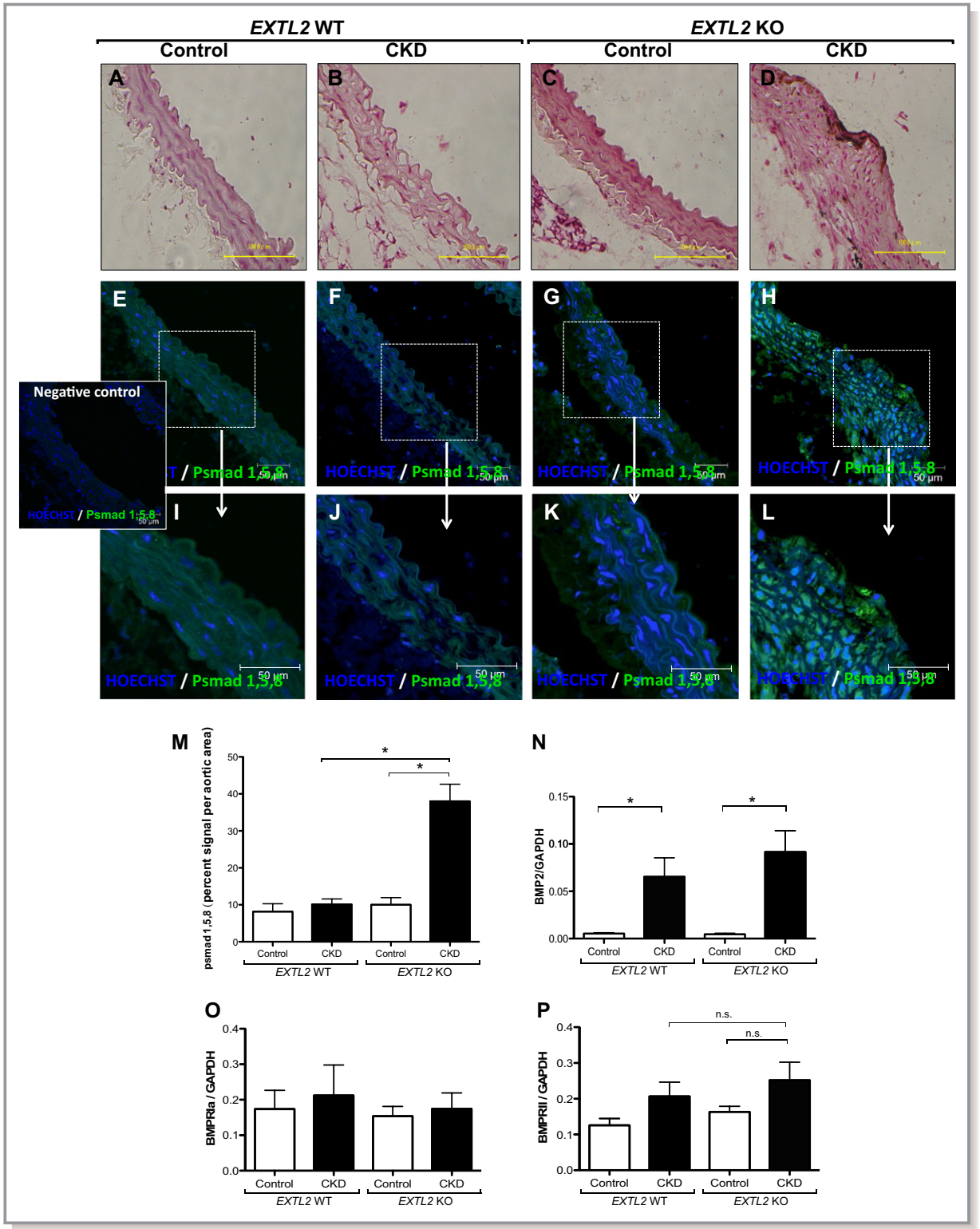

Figure 12. Activated BMP signaling in calcified aorta of *EXTL2* KO mice. Phosphorylated-smad 1/5/8 was enhanced in calcified aorta of *EXTL2* KO mice (H, L) but not in other groups (E through G, I through K). The phosphorylated-smad 1/5/8 signal was quantified and shown as percentage per aortic area (M). The mRNA expression of BMP2 ligands determined by qRT-PCR showed increased in both CKD groups. However, no significant different of BMP2 expression in CKD groups was found (N). We observed no differences in both BMP receptor type Ia (BMPRIa) and BMP receptor type II (BMPRII) (O and P). Data are presented as mean±SEM (n=4 to 5), **P*<0.05, ***P*<0.001, n.s., not significant by Mann-Whitney *U* test. BMP2 indicates bone morphogenetic protein 2; CKD, chronic kidney disease; *EXTL2* KO, *exostosin-like glycosyltransferase 2* knockout; GAPDH, glyceraldehyde-3-phosphate dehydrogenase; qRT-PCR, quantitative real-time polymerase chain reaction; WT, wild-type.

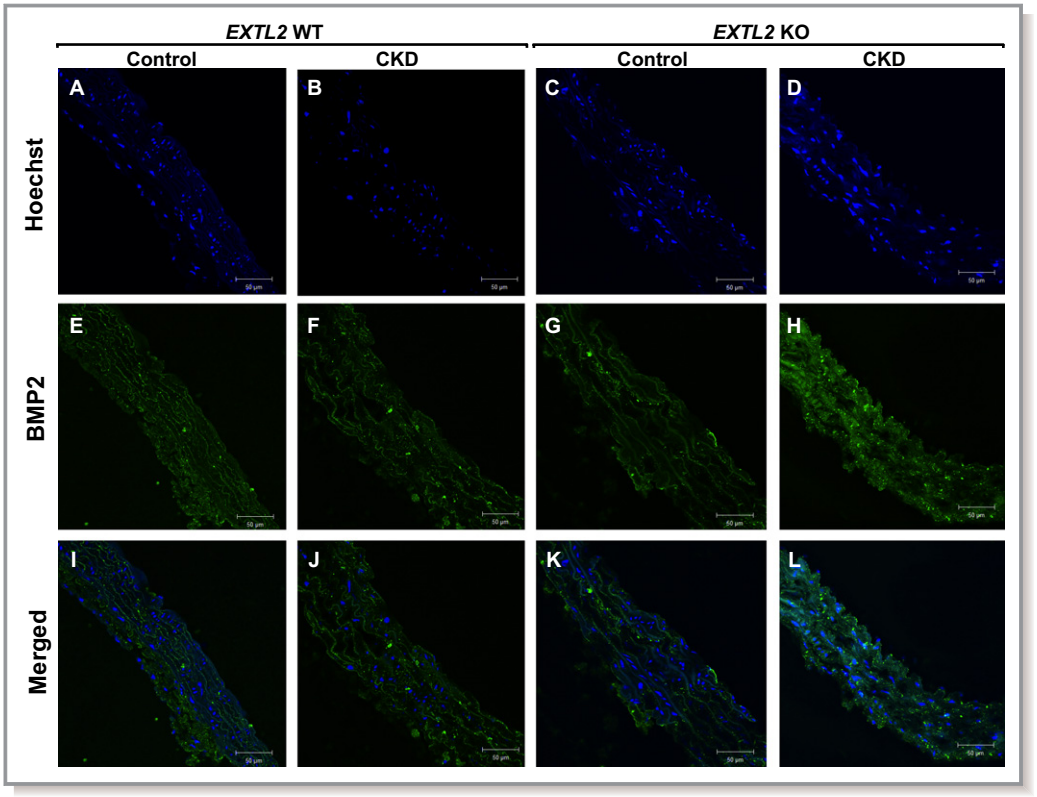

Figure 13. BMP2 accumulation in calcified aorta. Exogenous rhBMP2 was more abundantly trapped on calcified aorta (H, L) than WT CKD and both control groups (E through G, I through K). BMP2 indicates bone morphogenetic protein 2; CKD, chronic kidney disease; *EXTL2* KO, *exostosin-like glycosyltransferase 2* knockout; WT, wild-type.

Similarly; we detected high expression of runt-related transcription factor 2, an osteoblastic differentiation factor, and low expression of the VSMC markers smooth muscle–22α and α–smooth muscle actin in the calcified aorta. These findings suggest that under high-phosphate conditions, high HS and CS levels in the aortas of *EXTL2* KO mice accelerate vascular calcification by enhancing BMP2 signaling through p-smad1/5/8, which further induces phenotypic transition of VSMCs.

In addition, previous studies showed that sulfation pattern of glycosaminoglycan contributes in the various mechanisms.[49,50] In our study, we also measured the disaccharides composition and found that the 6-sulfation pattern, but not the 4-sulfation pattern, of CS in *EXTL2* KO mice is higher than those on *EXTL2* WT mice. During osteoblastic differentiation, CS-C, which consists of 6-*O*-sulfate at its *N*-acetylated hexosamine and hexuronic acid residues, activates p-smad1/5/8 expression. However, CS-E, which is enriched with 4-*O*-sulfate and 6-*O*-sulfate at its *N*-acetylated hexosamine and hexuronic acid residues, activates p-smad1/5/8 expression with higher level than CS-C.[36] Despite the modest role of 6-sulfation during osteoblast differentiation, the change of disaccharides composition in *EXTL2* KO mice may also contribute in the vascular calcification development. Nevertheless, further study is needed to elucidate the importance of 6-sulfation pattern during vascular calcification development.

In the in vitro study, we demonstrated that under high-phosphate conditions, overexpression of glycosaminoglycan enhanced calcium deposition in mouse VSMCs and that deletion of the cell surface and ECM HS or CS from mouse VSMCs effectively abrogated the calcification.

In conclusion, we are the first to demonstrate the importance of HS and CS in CKD-induced vascular calcification. Up-regulation of HS and CS in aortic tissue clearly accelerates the progression of vascular calcification in animals with CKD. Attenuation of HS or CS effectively reduces the calcium deposition in VSMCs under high-phosphate conditions. Considering the complexity of vascular calcification mechanisms, a balance between vascular calcification inducers and inhibitors is necessary. These results suggest that controlling HS and CS expression may help in preventing or inhibiting the progression of vascular calcification in CKD.

Sources of Funding

This study was supported by Ministry of Education, Culture, Sports, Science, and Technology (MEXT)–Supported Program

for the Strategic Research Foundation at Private Universities, 2012–2017 (to H.K.); The Science Research Promotion Fund from The Promotion and Mutual Aid Corporation for Private Schools of Japan (to N.E); Grant-in-Aid for Scientific Research in Innovative Areas 23110003 (Deciphering Sugar Chain–based Signals Regulating Integrative Neuronal Functions [to H.K.]) from MEXT, Japan; and Faculty Resources Grant, Kobe University, the Global COE Program, Global Center of Excellence for Education and Research on Signal Transduction Medicine in the Coming Generation from the Ministry of Education, Culture, Sports, Science, and Technology (MEXT) of Japan (to E.P).

Disclosures

None.

References

1. Herzog CA, Asinger RW, Berger AK, Charytan DM, Diez J, Hart RG, Eckardt KU, Kasiske BL, McCullough PA, Passman RS, DeLoach SS, Pun PH, Ritz E. Cardiovascular disease in chronic kidney disease. A clinical update from Kidney Disease: improving Global Outcomes (KDIGO). *Kidney Int*. 2011;80:572–586.
2. Aoki A, Kojima F, Uchida K, Tanaka Y, Nitta K. Associations between vascular calcification, arterial stiffness and bone mineral density in chronic hemodialysis patients. *Geriatr Gerontol Int*. 2009;9:246–252.
3. Jensky NE, Criqui MH, Wright MC, Wassel CL, Brody SA, Allison MA. Blood pressure and vascular calcification. *Hypertension*. 2010;55:990–997.
4. Miwa Y, Tsushima M, Arima H, Kawano Y, Sasaguri T. Pulse pressure is an independent predictor for the progression of aortic wall calcification in patients with controlled hyperlipidemia. *Hypertension*. 2004;43:536–540.
5. O'Neill WC, Lomashvili KA. Recent progress in the treatment of vascular calcification. *Kidney Int*. 2010;78:1232–1239.
6. Wolf M, Shah A, Gutierrez O, Ankers E, Monroy M, Tamez H, Steele D, Chang Y, Camargo CA Jr, Tonelli M, Thadhani R. Vitamin D levels and early mortality among incident hemodialysis patients. *Kidney Int*. 2007;72:1004–1013.
7. Raggi P, Chertow GM, Torres PU, Csiky B, Naso A, Nossuli K, Moustafa M, Goodman WG, Lopez N, Downey G, Dehmel B, Floege J. The ADVANCE study: a randomized study to evaluate the effects of cinacalcet plus low-dose vitamin D on vascular calcification in patients on hemodialysis. *Nephrol Dial Transplant*. 2011;26:1327–1339.
8. Takei T, Otsubo S, Uchida K, Matsugami K, Mimuro T, Kabaya T, Akiba T, Nitta K. Effects of sevelamer on the progression of vascular calcification in patients on chronic haemodialysis. *Nephron Clin Pract*. 2008;108:278–283.
9. Hutchison AJ, Smith CP, Brenchley PE. Pharmacology, efficacy and safety of oral phosphate binders. *Nat Rev Nephrol*. 2011;7:578–589.
10. Ikee R, Tsunoda M, Sasaki N, Sato N, Hashimoto N. Emerging effects of sevelamer in chronic kidney disease. *Kidney Blood Press Res*. 2013;37:24–32.
11. Wu M, Rementer C, Giachelli CM. Vascular calcification: an update on mechanisms and challenges in treatment. *Calcif Tissue Int*. 2013;1:1–9.
12. Checherita IA, Smarandache D, David C, Ciocalteu A, Ion DA, Lascar I. Vascular calcifications in chronic kidney disease-clinical management. *Rom J Morphol Embryol*. 2012;53:7–13.
13. Bostrom K, Watson KE, Horn S, Wortham C, Herman IM, Demer LL. Bone morphogenetic protein expression in human atherosclerotic lesions. *J Clin Invest*. 1993;91:1800–1809.
14. Speer MY, Yang HY, Brabb T, Leaf E, Look A, Lin WL, Frutkin A, Dichek D, Giachelli CM. Smooth muscle cells give rise to osteochondrogenic precursors and chondrocytes in calcifying arteries. *Circ Res*. 2009;104:733–741.
15. Steitz SA, Speer MY, Curinga G, Yang HY, Haynes P, Aebersold R, Schinke T, Karsenty G, Giachelli CM. Smooth muscle cell phenotypic transition associated with calcification: upregulation of Cbfa1 and downregulation of smooth muscle lineage markers. *Circ Res*. 2001;89:1147–1154.
16. Chen NX, O'Neill KD, Duan D, Moe SM. Phosphorus and uremic serum up-regulate osteopontin expression in vascular smooth muscle cells. *Kidney Int*. 2002;62:1724–1731.
17. Lomashvili KA, Wang X, Wallin R, O'Neill WC. Matrix Gla protein metabolism in vascular smooth muscle and role in uremic vascular calcification. *J Biol Chem*. 2011;286:28715–28722.
18. Veis A. Mineral-matrix interactions in bone and dentin. *J Bone Miner Res*. 1993;8:493–497.
19. McQuillan DJ, Richardson MD, Bateman JF. Matrix deposition by a calcifying human osteogenic sarcoma cell line (SAOS-2). *Bone*. 1995;16:415–426.
20. Watson KE, Parhami F, Shin V, Demer LL. Fibronectin and collagen I matrixes promote calcification of vascular cells in vitro, whereas collagen IV matrix is inhibitory. *Arterioscler Thromb Vasc Biol*. 1998;18:1964–1971.
21. Fischer JW, Steitz SA, Johnson PY, Burke A, Kolodgie F, Virmani R, Giachelli C, Wight TN. Decorin promotes aortic smooth muscle cell calcification and colocalizes to calcified regions in human atherosclerotic lesions. *Arterioscler Thromb Vasc Biol*. 2004;24:2391–2396.
22. Luo G, Ducy P, McKee MD, Pinero GJ, Loyer E, Behringer RR, Karsenty G. Spontaneous calcification of arteries and cartilage in mice lacking matrix GLA protein. *Nature*. 1997;386:78–81.
23. Stephens EH, Saltarrelli JG, Baggett LS, Nandi I, Kuo JJ, Davis AR, Olmsted-Davis EA, Reardon MJ, Morrisett JD, Grande-Allen KJ. Differential proteoglycan and hyaluronan distribution in calcified aortic valves. *Cardiovasc Pathol*. 2011;20:334–342.
24. Bishop JR, Schuksz M, Esko JD. Heparan sulphate proteoglycans fine-tune mammalian physiology. *Nature*. 2007;446:1030–1037.
25. Nadanaka S, Kitagawa H. Heparan sulphate biosynthesis and disease. *J Biochem*. 2008;144:7–14.
26. Afratis N, Gialeli C, Nikitovic D, Tsegenidis T, Karousou E, Theocharis AD, Pavao MS, Tzanakakis GN, Karamanos NK. Glycosaminoglycans: key players in cancer cell biology and treatment. *FEBS J*. 2012;279:1177–1197.
27. Kuo WJ, Digman MA, Lander AD. Heparan sulfate acts as a bone morphogenetic protein coreceptor by facilitating ligand-induced receptor hetero-oligomerization. *Mol Biol Cell*. 2010;21:4028–4041.
28. Hu Z, Wang C, Xiao Y, Sheng N, Chen Y, Xu Y, Zhang L, Mo W, Jing N, Hu G. NDST1-dependent heparan sulfate regulates BMP signaling and internalization in lung development. *J Cell Sci*. 2009;122:1145–1154.
29. Adhikari N, Carlson M, Lerman B, Hall JL. Changes in expression of proteoglycan core proteins and heparan sulfate enzymes in the developing and adult murine aorta. *J Cardiovasc Transl Res*. 2011;4:313–320.
30. Tran-Lundmark K, Tran PK, Paulsson-Berne G, Friden V, Soininen R, Tryggvason K, Wight TN, Kinsella MG, Boren J, Hedin U. Heparan sulfate in perlecan promotes mouse atherosclerosis: roles in lipid permeability, lipid retention, and smooth muscle cell proliferation. *Circ Res*. 2008;103:43–52.
31. Wight TN, Merrilees MJ. Proteoglycans in atherosclerosis and restenosis: key roles for versican. *Circ Res*. 2004;94:1158–1167.
32. Duncan GC, McCormick C, Tufaro F. The link between heparan sulfate and hereditary bone disease: finding a function for the EXT family of putative tumor suppressor proteins. *J Clin Invest*. 2001;108:511–516.
33. Cortes M, Baria AT, Schwartz NB. Sulfation of chondroitin sulfate proteoglycans is necessary for proper Indian hedgehog signaling in the developing growth plate. *Development*. 2009;136:1697–1706.
34. Bramono DS, Murali S, Rai B, Ling L, Poh WT, Lim ZX, Stein GS, Nurcombe V, van Wijnen AJ, Cool SM. Bone marrow-derived heparan sulfate potentiates the osteogenic activity of bone morphogenetic protein-2 (BMP-2). *Bone*. 2012;50:954–964.
35. Buttner M, Keller M, Huster D, Schiller J, Schnabelrauch M, Dieter P, Hempel U. Over-sulfated chondroitin sulfate derivatives induce osteogenic differentiation of hMSC independent of BMP-2 and TGF-beta1 signalling. *J Cell Physiol*. 2013;228:330–340.
36. Koike T, Izumikawa T, Tamura J, Kitagawa H. Chondroitin sulfate-E fine-tunes osteoblast differentiation via ERK1/2, Smad3 and Smad1/5/8 signaling by binding to N-cadherin and cadherin-11. *Biochem Biophys Res Commun*. 2012;420:523–529.
37. Nadanaka S, Zhou S, Kagiyama S, Shoji N, Sugahara K, Sugihara K, Asano M, Kitagawa H. *EXTL2*, a member of EXT family of tumor suppressors, controls glycosaminoglycan biosynthesis in a xylose kinase-dependent manner. *J Biol Chem*. 2013;288:9321–9333.
38. Miyazaki-Anzai S, Levi M, Kratzer A, Ting TC, Lewis LB, Miyazaki M. Farnesoid X receptor activation prevents the development of vascular calcification in ApoE-/- mice with chronic kidney disease. *Circ Res*. 2010;106:1807–1817.
39. Ray JL, Leach R, Herbert JM, Benson M. Isolation of vascular smooth muscle cells from a single murine aorta. *Methods Cell Sci*. 2001;23:185–188.

40. DeBiasio R, Bright GR, Ernst LA, Waggoner AS, Taylor DL. Five-parameter fluorescence imaging: wound healing of living Swiss 3T3 cells. *J Cell Biol*. 1987;105:1613–1622.
41. Okada M, Nadanaka S, Shoji N, Tamura J, Kitagawa H. Biosynthesis of heparan sulfate in EXT1-deficient cells. *Biochem J*. 2010;428:463–471.
42. Wuyts W, Van Hul W, Hendrickx J, Speleman F, Wauters J, De Boulle K, Van Roy N, Van Agtmael T, Bossuyt P, Willems PJ. Identification and characterization of a novel member of the EXT gene family, *EXTL2*. *Eur J Hum Genet*. 1997;5:382–389.
43. Nadanaka S, Kagiyama S, Kitagawa H. *EXTL2*, a member of EXT family of tumor suppressors, in liver injury and regeneration processes. *Biochem J*. 2013; 454:133–145.
44. Qiao JH, Xie PZ, Fishbein MC, Kreuzer J, Drake TA, Demer LL, Lusis AJ. Pathology of atheromatous lesions in inbred and genetically engineered mice. Genetic determination of arterial calcification. *Arterioscler Thromb*. 1994;14:1480–1497.
45. McEniery CM, McDonnell BJ, So A, Aitken S, Bolton CE, Munnery M, Hickson SS, Yasmin, Maki-Petaja KM, Cockcroft JR, Dixon AK, Wilkinson IB. Aortic calcification is associated with aortic stiffness and isolated systolic hypertension in healthy individuals. *Hypertension*. 2009;53:524–531.
46. Rattazzi M, Bertacco E, Puato M, Faggin E, Pauletto P. Hypertension and vascular calcification: a vicious cycle? *J Hypertens*. 2012;30:1885–1893.
47. Koleganova N, Piecha G, Ritz E, Schirmacher P, Muller A, Meyer HP, Gross ML. Arterial calcification in patients with chronic kidney disease. *Nephrol Dial Transplant*. 2009;24:2488–2496.
48. Li X, Yang HY, Giachelli CM. BMP-2 promotes phosphate uptake, phenotypic modulation, and calcification of human vascular smooth muscle cells. *Atherosclerosis*. 2008;199:271–277.
49. Miyata S, Komatsu Y, Yoshimura Y, Taya C, Kitagawa H. Persistent cortical plasticity by upregulation of chondroitin 6-sulfation. *Nat Neurosci*. 2012; 15:414–422.
50. Garg HG, Yu L, Hales CA, Toida T, Islam T, Linhardt RJ. Sulfation patterns in heparin and heparan sulfate: effects on the proliferation of bovine pulmonary artery smooth muscle cells. *Biochim Biophys Acta*. 2003;1639: 225–231.